Dufour and Soret effects on unsteady free convective flow past a semi infinite vertical plate with variable viscosity and thermal conductivity

P. Loganathan[1], D. Iranian[2], P. Ganesan[3]

[1, 3]Department of Mathematics, Anna University, Chennai – 600025, India
Email: [1] logu@annauniv.edu, Email: [3]ganesan@annauniv.edu
[2]Department of Mathematics, Panimalar Institute of Technology, Chennai – 600123, India
Email: [2] mdiranian74@gmail.com

Abstract: An analysis is performed to study the influence of temperature-dependent viscosity and thermal conductivity on the unsteady laminar free convection flow over a semi infinite vertical plate by taking into account the Dufour and Soret numbers. Both viscosity and thermal conductivity are variables and considered only a function of temperature. It is assumed that the viscosity of the fluid is an exponential function and thermal conductivity is a linear function of the temperature. The non-linear coupled dimensionless equations governing the boundary layer flow, heat and mass transfer are solved by using implicit finite-difference method of Crank-Nicolson type. An analysis of the effects of different parameters on dimensionless velocity, temperature and concentration profiles, as well as the local and average skin-friction and the rates of heat and mass transfer, is shown graphically.

Keywords: Dufour and Soret numbers, variable viscosity, thermal conductivity, unsteady, vertical plate

I. INTRODUCTION

The phenomenon of free convection by the simultaneous action of buoyancy forces from thermal and mass diffusion has many industrial applications such as in cooling a nuclear reactor, geothermal systems, oceanography and granular insulation, chemical, drying processes and solidification of binary alloy etc. A number of investigations have already been carried out with combined heat and mass transfer under the assumption of different physical situations. When heat and mass transfer occur simultaneously between the fluxes, the driving potentials are of more intricate nature. An energy flux can be generated not only by temperature gradients but by composition gradients. The energy flux caused by a composition is called Dufour or diffusion-thermo effect. Temperature gradients can also create mass fluxes, and this is the Soret or thermal-diffusion effect. Both effects have been extensively studied in gases and the Soret effect has been studied both theoretically and experimentally in liquids. Sparrow et al. [1] studied experimentally the effect of diffusion thermo on the heat transfer, mass transfer, and flow in a boundary layer into which various foreign gases are injected.

Generally, the thermal-diffusion and the diffusion thermo effects are of a smaller-order magnitude than the effects prescribed by Fourier's or Fick's laws and are often neglected in heat and mass transfer processes. Mass transfer is one of the most commonly encountered phenomena in chemical industries as well as in physical and biological sciences. When mass transfer takes place in a fluid at rest, the mass is transferred purely by molecular diffusion resulting from concentration gradients. For low concentrations of the mass in the fluid and low mass transfer rates, the convective heat and mass transfer process are similar in nature. Gnaneswara Reddy and Bhaskar Reddy [2] analyzed a steady two-dimensional MHD free convection flow viscous dissipating fluid past a semi-infinite moving vertical plate in a porous medium with Soret and Dufour effects using Runge-Kutta fourth order with shooting method, the velocity decreases with an increase in the magnetic parameter. Alam et al. [3] have analyzed numerically the Dufour and Soret effects on combined free-forced convection and mass transfer flow past a semi-infinite vertical plate, under the influence of a transversely applied magnetic field. The thermal diffusion and the diffusion-thermo effects on a steady laminar boundary layer flow over a vertical flat plate with temperature dependent viscosity, was studied by Kafoussias and Williams [4]. Many researchers, Postelnicu [5], Alam et al. [6] and Hayat et al. [7] have considered the Dufour and Soret effects on natural convection heat and mass transfer over a vertical surface in a porous medium extensively. Srinivasacharya and Ram [8] presented the Soret and Dufour Effects on mixed convection heat and mass transfer in a micropolar fluid using the Keller-box method. These problems are solved without the parameters of variable viscosity and thermal conductivity using different methods but not implicit finite-difference method of Crank-Nicolson type.

The term viscosity is essential in the field of fluid flow. However, the variation of viscosity with temperature is an interesting macroscopical physical phenomenon in fluid mechanics. It is necessary to consider

the variation of viscosity in the fluid flow problems to accurately predict the flow behaviour. Kafoussias and Williams [9] presented the effect of temperature dependent viscosity on free-forced convective laminar boundary layer flow past a vertical isothermal flat plate. Hady et al. [10] studied mixed convection boundary layer flow on a continuous flat plate with variable viscosity. Eldahab and Salem [11] investigated the radiation effect in the presence of a uniform transverse magnetic field on steady free convection flow with variable viscosity is investigated. The fluid viscosity is assumed to vary as the reciprocal of a linear function of temperature and the governing equations were solved by shooting method. The effects of variable viscosity on hydromagnetic flow and heat transfer past a continuously moving porous boundary with radiation have been studied by Seddeek [12]. Hossain et al. [13] investigated the effect of radiation on the free convection flow of fluid with variable viscosity from a porous vertical plate. Using the Chebyshev finite-difference method, Elbarbary and Elgazery [14] investigated the effects of variable viscosity and variable thermal conductivity on heat transfer from moving surfaces with radiation. Rahman et al. [15] presented the effects of temperature dependent thermal conductivity on magneto hydrodynamic (MHD) free convection flow along a vertical flat plate with heat conduction. Mahanti and Gaur [16] studied the effects of varying viscosity and thermal conductivity on steady free convective flow and heat transfer along an isothermal vertical plate in the presence of a heat sink.

These problems are analyzed in the absence of the effects of the Dufour and Soret numbers. Therefore, the objective of this study is to investigate the heat and mass transfer by natural convection from a semi infinite vertical plate, considering the Dufour and Soret effects with variable viscosity and thermal conductivity.

II. MATHEMATICAL FORMULATION

Consider a two dimensional unsteady flow of a viscous, incompressible fluid past a semi-infinite vertical plate, taking into account the Soret and Dufour effects. Both the Dufour and Soret effects are considered when the fluid is not chemically reacting. Assume that the *x*-axis is taken along the plate in the vertically upward direction and the *y*-axis is chosen normal to the plate as shown in Fig.1. The gravitational acceleration is acting downward. The surrounding stationary fluid temperature is assumed to be of the ambient temperature T_∞. Initially, it is assumed that the plate and the fluid are at the same ambient temperature T_∞. As time increases, the temperature of the plate is suddenly raised to T_w ($> T_\infty$) and is maintained at the same value. It is assumed that the effect of viscous dissipation is negligible in the energy equation. All the fluid physical properties are assumed to be constant except for the fluid viscosity, which varies exponentially with the fluid temperature, the thermal conductivity which varies linearly with the fluid temperature.

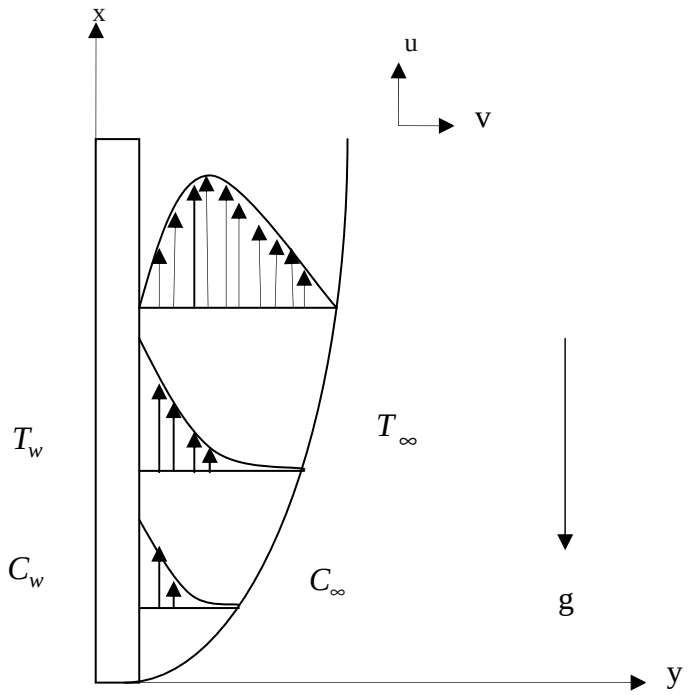

Fig. 1: Flow model of the problem

Under these assumptions, the governing boundary layer equations of continuity, momentum and energy and mass with Boussinesq's approximation are as follows (Eckert and Drake [17], Schlichting [18]):

$$\frac{\partial u}{\partial x}+\frac{\partial v}{\partial y}=0 \tag{1}$$

$$\frac{\partial u}{\partial t'}+u\frac{\partial u}{\partial x}+v\frac{\partial u}{\partial y}=\frac{1}{\rho}\frac{\partial}{\partial y}\left(\mu\frac{\partial u}{\partial y}\right)+g\beta(T-T_\infty)+g\beta^*(c'-c'_\infty) \tag{2}$$

$$\frac{\partial T}{\partial t'}+u\frac{\partial T}{\partial x}+v\frac{\partial T}{\partial y}=\frac{1}{\rho C_p}\frac{\partial}{\partial y}\left(k\frac{\partial T}{\partial y}\right)+\frac{D_m k_T}{C_s C_p}\left(\frac{\partial^2 c'}{\partial y^2}\right) \tag{3}$$

$$\frac{\partial c'}{\partial t'}+u\frac{\partial c'}{\partial x}+v\frac{\partial c'}{\partial y}=D_m\frac{\partial^2 c'}{\partial y^2}+\frac{D_m k_T}{T_m}\frac{\partial^2 T}{\partial y^2} \tag{4}$$

The initial and boundary conditions are

$$\begin{aligned} &t'\le 0:\ u=0,\ \ v=0,\ \ T=T_\infty,\ \ c'=c'_\infty \quad \text{for all x and y}\\ &t'>0:\ u=0,\ \ v=0,\ \ T=T_w,\ \ c'=c'_w \quad \text{at}\ \ \mathrm{y}=0\\ &\qquad u=0,\ \ v=0,\ \ T=T_\infty,\ \ c'=c'_\infty \quad \text{at}\ \ \mathrm{x}=0\\ &\qquad u\to 0,\ T\to T_\infty,\ \ c'\to c'_\infty \quad \text{as}\ \ \mathrm{y}\to\infty \end{aligned} \tag{5}$$

Introducing the following non dimensional quantities

$$\begin{aligned} &X=\frac{x}{L},\ Y=\frac{yGr^{1/4}}{L},\ U=\frac{uLGr^{-1/2}}{\upsilon},\ V=\frac{vLGr^{-1/4}}{\upsilon},\ t=\frac{t'\upsilon Gr^{1/2}}{L^2},\\ &\theta=\frac{T-T_\infty}{T_w-T_\infty},\ C=\frac{c'-c'_\infty}{c'_w-c'_\infty},\ Gr=\frac{g\beta L^3\left(T_w-T_\infty\right)}{\upsilon^2},\ N=\frac{\beta^*(c'_w-c'_\infty)}{\beta\left(T_w-T_\infty\right)},\\ &Du=\frac{D_m k_T}{\upsilon c_s c_p}\frac{(c'_w-c'_\infty)}{\left(T_w-T_\infty\right)},\ Sr=\frac{D_m k_T}{\upsilon T_m}\frac{\left(T_w-T_\infty\right)}{(c'_w-c'_\infty)},\ Pr=\frac{\upsilon\rho c_p}{k_\infty},\ Sc=\frac{\upsilon}{D} \end{aligned} \tag{6}$$

The variations of the normalized viscosity and thermal conductivity are written in the form (Elbashbeshy and Ibrahim [19] and Ockendon and Ockendon [20]):

$$\mu(\theta)=\mu_\infty exp(-\lambda\theta),\qquad k(\theta)=k_\infty(1+\gamma\theta) \tag{7}$$

The reduced equations of (1) to (4) by introducing the non-dimensional quantities are

$$\frac{\partial U}{\partial X}+\frac{\partial V}{\partial Y}=0 \tag{8}$$

$$\frac{\partial U}{\partial t}+U\frac{\partial U}{\partial X}+V\frac{\partial U}{\partial Y}=exp(-\lambda\theta)\left(\frac{\partial^2 U}{\partial Y^2}-\lambda\frac{\partial U}{\partial Y}\frac{\partial\theta}{\partial Y}\right)+\theta+NC \tag{9}$$

$$\frac{\partial\theta}{\partial t}+U\frac{\partial\theta}{\partial X}+V\frac{\partial\theta}{\partial Y}=\frac{1}{Pr}\left[(1+\gamma\theta)\frac{\partial^2\theta}{\partial Y^2}+\gamma\left(\frac{\partial\theta}{\partial Y}\right)^2\right]+Du\frac{\partial^2 C}{\partial Y^2} \tag{10}$$

$$\frac{\partial C}{\partial t}+U\frac{\partial C}{\partial X}+V\frac{\partial C}{\partial Y}=\frac{1}{Sc}\frac{\partial^2 C}{\partial Y^2}+Sr\frac{\partial^2\theta}{\partial Y^2} \tag{11}$$

The corresponding initial and boundary conditions of (5) are

$$\begin{aligned} t \le 0: &\quad U = 0,\ V = 0,\ \theta = 0,\ C = 0 \quad \text{for all X and Y} \\ t > 0: &\quad U = 0,\ V = 0,\ \theta = 1,\ C = 1 \quad \text{at} \quad \mathrm{Y} = 0 \\ &\quad U = 0,\ V = 0,\ \theta = 0,\ C = 0 \quad \text{at} \quad \mathrm{X} = 0 \\ &\quad U \to 0,\quad \theta \to 0,\quad C \to 0 \qquad \text{as} \quad \mathrm{Y} \to \infty \end{aligned} \tag{12}$$

III. NUMERICAL TECHNIQUE

The governing equations (8) to (11) are unsteady, coupled and non-linear with initial and boundary conditions. The following implicit finite-difference method of the Crank-Nicolson type is used to solve the governing equations. The corresponding finite-difference equations [Ramachandra Prasad et al. [21] are

$$\frac{U_{i,j}^{n+1} - U_{i-1,j}^{n+1} + U_{i,j}^{n} - U_{i-1,j}^{n} + U_{i,j-1}^{n+1} - U_{i-1,j-1}^{n+1} + U_{i,j-1}^{n} - U_{i-1,j-1}^{n}}{4\Delta X} + \frac{V_{i,j}^{n+1} - V_{i,j-1}^{n+1} + V_{i,j}^{n} - V_{i,j-1}^{n}}{2\Delta Y} = 0$$

$$\frac{U_{i,j}^{n+1} - U_{i,j}^{n}}{\Delta t} + U_{i,j}^{n}\left[\frac{U_{i,j}^{n+1} - U_{i-1,j}^{n+1} + U_{i,j}^{n} - U_{i-1,j}^{n}}{2\Delta X}\right] + V_{i,j}^{n}\left[\frac{U_{i,j+1}^{n+1} - U_{i,j-1}^{n+1} + U_{i,j+1}^{n} - U_{i,j-1}^{n}}{4\Delta Y}\right]$$

$$= \left(\frac{\theta_{i,j}^{n+1} + \theta_{i,j}^{n}}{2}\right) + exp\,(-\lambda\theta)\quad \left[\frac{U_{i,j-1}^{n+1} - 2U_{i,j}^{n+1} + U_{i,j+1}^{n+1} + U_{i,j-1}^{n} - 2U_{i,j}^{n} + U_{i,j+1}^{n}}{2(\Delta Y)^2}\right]$$

$$- \lambda\, exp(\lambda\theta)\quad \left[\frac{U_{i,j+1}^{n+1} - U_{i,j-1}^{n+1} + U_{i,j+1}^{n} - U_{i,j-1}^{n}}{4\Delta Y}\right]\left[\frac{\theta_{i,j+1}^{n+1} - \theta_{i,j-1}^{n+1} + \theta_{i,j+1}^{n} - \theta_{i,j-1}^{n}}{4\Delta Y}\right]$$

$$+ N\left(\frac{C_{i,j}^{n+1} + C_{i,j}^{n}}{2}\right)$$

$$\frac{\theta_{i,j}^{n+1} - \theta_{i,j}^{n}}{\Delta t} + U_{i,j}^{n}\left[\frac{\theta_{i,j}^{n+1} - \theta_{i-1,j}^{n+1} + \theta_{i,j}^{n} - \theta_{i-1,j}^{n}}{2\Delta X}\right] + V_{i,j}^{n}\left[\frac{\theta_{i,j+1}^{n+1} - \theta_{i,j-1}^{n+1} + \theta_{i,j+1}^{n} - \theta_{i,j-1}^{n}}{4\Delta Y}\right]$$

$$= \frac{1}{Pr}\left[\left(1 + \gamma\left(\frac{\theta_{i,j}^{n+1} + \theta_{i,j}^{n}}{2}\right)\right)\left(\frac{\theta_{i,j-1}^{n+1} - 2\theta_{i,j}^{n+1} + \theta_{i,j+1}^{n+1} + \theta_{i,j-1}^{n} - 2\theta_{i,j}^{n} + \theta_{i,j+1}^{n}}{2(\Delta Y)^2}\right)\right]$$

$$+ \frac{\gamma}{Pr}\left(\frac{\theta_{i,j+1}^{n+1} - \theta_{i,j-1}^{n+1}}{2\Delta Y}\right)\left(\frac{\theta_{i,j+1}^{n} - \theta_{i,j-1}^{n}}{2\Delta Y}\right) + Du\left[\frac{C_{i,j-1}^{n+1} - 2C_{i,j}^{n+1} + C_{i,j+1}^{n+1} + C_{i,j-1}^{n} - 2C_{i,j}^{n} + C_{i,j+1}^{n}}{2(\Delta Y)^2}\right]$$

$$\frac{C_{i,j}^{n+1} - C_{i,j}^{n}}{\Delta t} + U_{i,j}^{n}\left[\frac{C_{i,j}^{n+1} - C_{i-1,j}^{n+1} + C_{i,j}^{n} - C_{i-1,j}^{n}}{2\Delta X}\right] + V_{i,j}^{n}\left[\frac{C_{i,j+1}^{n+1} - C_{i,j-1}^{n+1} + C_{i,j+1}^{n} - C_{i,j-1}^{n}}{4\Delta Y}\right]$$

$$= \frac{1}{Sc}\left[\frac{C_{i,j-1}^{n+1} - 2C_{i,j}^{n+1} + C_{i,j+1}^{n+1} + C_{i,j-1}^{n} - 2C_{i,j}^{n} + C_{i,j+1}^{n}}{2(\Delta Y)^2}\right]$$

$$+ Sr\left(\frac{\theta_{i,j-1}^{n+1} - 2\theta_{i,j}^{n+1} + \theta_{i,j+1}^{n+1} + \theta_{i,j-1}^{n} - 2\theta_{i,j}^{n} + \theta_{i,j+1}^{n}}{2(\Delta Y)^2}\right)$$

The solution domain, considered as a rectangle consists of grid points at which the discretization equations are applied. In this domain, by definition of the non dimensional quantity X, assumed in equation (6), X varies from 0 to 1, where $X = 1$ corresponds to the height of the plate. But the choice of value of Y, corresponding to $Y = \infty$, has an important influence of the solution. The effect of different values to represent $Y = \infty$ on numerical scheme has been investigated and it is concluded that the value of $Y_{max} = 20$ is sufficiently large. Further larger values of Y produced the results with indistinguishable difference, where Y_{max} corresponds to $Y = \infty$, which lies well outside both the momentum and energy boundary layers. The maximum of Y was chosen as 20, after some preliminary investigations so that the last two boundary conditions of (12) are satisfied.

During any one time-step, the coefficients $U_{i,j}^{n}, V_{i,j}^{n}$ appearing in the scheme of finite difference equations of (8) to (11) are treated as constants, where the subscript *i* designates the grid point along *X* direction, *j* designates the grid point along *Y* direction and the superscript *n* along *t* direction. An appropriate mesh size considered for the calculation is $\Delta X = 0.02$, $\Delta Y = 0.20$ and time step $\Delta t = 0.01$. The values of *U*, *V*, θ, and *C* are known at all grid points at $t = 0$ from the initial conditions. The values of *U*, *V*, θ, and *C* at time level (n+1) using the known values at previous level (n) are calculated as follows: The finite-difference scheme of the equation (11) at every internal node point on a particular *i*-level constitute a tridiagonal system of equations which is solved by Thomas algorithm, as described in Carnahan et al. [22]. Thus the values of *C* are found at every nodal point on a particular *i* at time level (n+1). Similarly the values of θ are calculated from the finite-difference equation of (10). Using the values of *C* and θ at time level (n+1), the values of *U* are found from the finite-difference scheme of the Equation (9) in a similar manner. Thus the values of *C*, θ and *U* are known on a particular *i*-level. The values of *V* are calculated explicitly using the finite-difference equation of (8) at every nodal point on a particular *i*-level at time level (n+1). This process is repeated for various *i*-levels. Thus the values of *C*, θ, *U* and *V* are known at all grid points in the rectangular region at time level (n+1). Computations are carried out until the steady-state is reached. The steady state solution is assumed to have been reached, when the absolute difference between the values of *U* as well as temperature θ and concentration *C* at two consecutive time steps are less than 10^{-5} at all grid points.

The scheme is proved to be unconditionally stable by using the von-Neumann technique, as shown by Soundalgekar and Ganesan [23]. The local truncation error is $O(\Delta t^2 + \Delta X + \Delta Y^2)$, and it tends to zero as Δt, ΔX, and ΔY tend to zero. Hence, the scheme is compatible. The stability and compatibility ensure the convergence of the scheme.

IV. RESULTS AND DISCUSSION

To get an insight into the physical situation of the problem, the values of velocity, temperature and concentration are calculated numerically for the different values of dimensionless parameters. The dimensionless numbers Du (Dufour number) and Sr (Soret number) which represent the diffusion-thermo and thermal-diffusion effects respectively, can take by their definition, arbitrary values, provided the value of their product is kept constant. The influences of the dimensionless parameters *Du*, *Sr*, λ, and γ on the flow field are analyzed for *Pr* = 0.71 (air), *Pr* = 7.0 (water), *Sc* = 0.22, and *N* = 5.0.

The simulated results are presented to outline the physics involved in the effects of varying *Du*, *Sr*, λ, γ and *Pr* on the transient velocity, temperature and concentration profiles during transient and steady-state periods. Initially, the velocity profiles with value zero at the wall, reach their temporal maximum very close to the wall, and then decrease to zero as *Y* becomes large for all time *t*. The velocity profiles are much thinner for higher values of Prandtl number, because the velocity diffusion extends far from the wall. The dimensionless velocity profiles in the boundary layer for different parameters λ, γ, *Du* and *Sr* for air and water, are presented in Figs.2 to 4. It is observed that the velocity increases, reaches the temporal maximum near the wall of the plate as the *Sr* increases, and then decays the free stream velocity. At the initial transient dimensionless velocity, the buoyancy-induced flow velocity is relatively low.

Fig. 2 shows that for cooling of the plate the velocity increases as the Soret number (*Sr*) increases. For example, when λ= 0.6, γ = 0.16, *Du* = 0.03, *Sr* = 2.0, *Pr* = 0.71, the velocity increases from the value zero at the wall, reaches the temporal maximum (*U* = 1.29821) at *t* = 12 very close to the wall and then slightly decreases monotonically to zero as *Y* becomes large for all time. It is observed that the time to reach the temporal maximum of the velocity and steady state decreases with increasing Soret number. This factor causes a decrease in the buoyancy force which decelerates the velocity of the flow. In Fig. 3, it is to be noted that with an increasing *Du*, the time to reach the temporal maximum (*U* = 1.04546) of the velocity increases, and then the velocity decreases to reach zero, whereas the time taken to reach the steady state are shown. In the steady state, the velocity increases as *Du* increases with time increasing. Fig. 4 shows the velocity profiles for different values of λ and γ, the velocity increases very closer to the wall and reaches the temporal maximum (*U* = 0.99674), and then decreases to zero. It is observed that the time to reach the temporal maximum and steady state increases with increasing λ and γ for air, with fixed values of *Du* = 0.12 and *Sr* = 0.5.

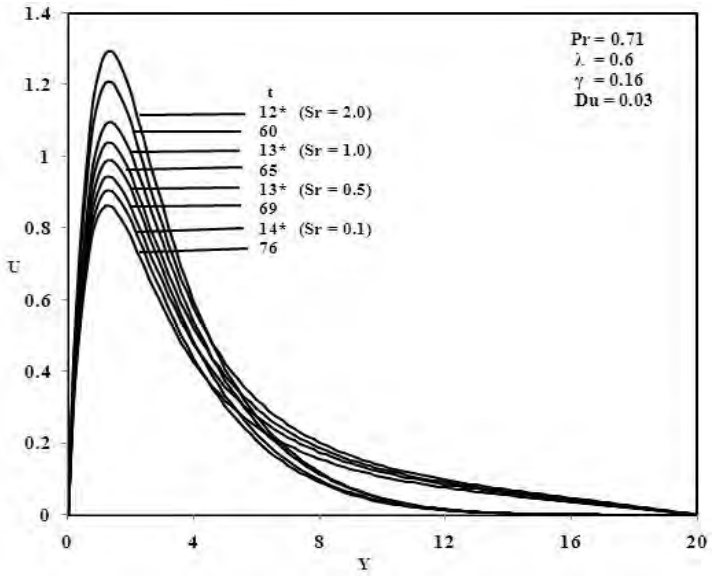

Fig. 2: Velocity profile for different values of Sr (* Temporal Maximum)

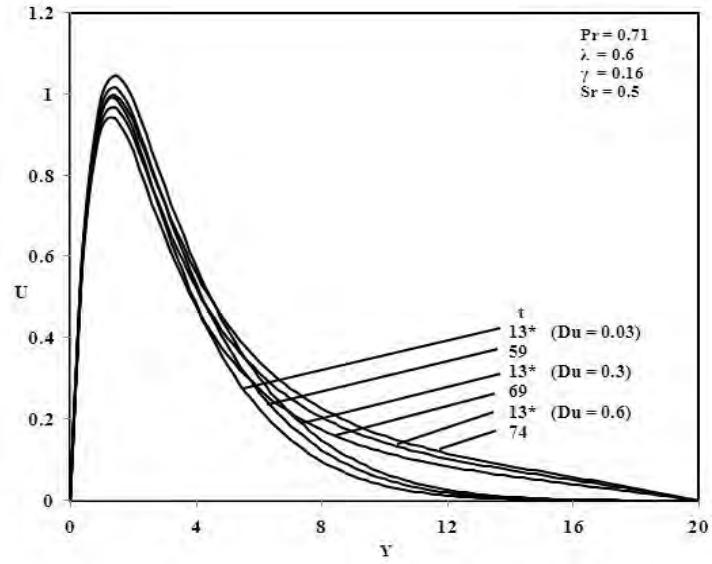

Fig. 3: Velocity profile for different values of Du (* Temporal Maximum)

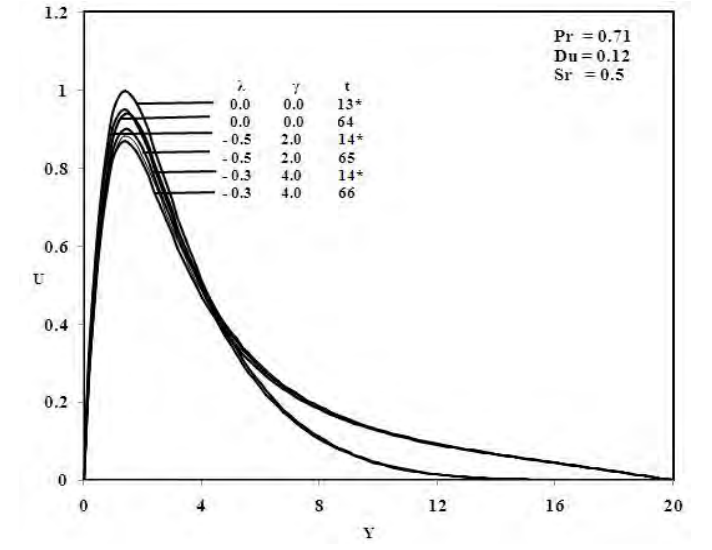

Fig. 4: Velocity profile for different values for λ and γ (* Temporal Maximum)

Figures 5 to 8 depict the steady state temperature profiles for different parameters. It can be observed that at the beginning there is no difference in the temperature profiles, with respect to time. Fig. 5 depicts that an increase in Sr results in decreasing the temperature profiles within the boundary layer, as well as the boundary layer thickness.

The steady state temperature profiles for air and for the fixed values of $\lambda = 0.6$, $\gamma = 0.16$ and Sr = 0.5 are shown in Fig. 6. The decreasing value of Du affects the temperature decreasing in the boundary layer. From Fig. 7, it is observed that the temperature decreases as the values of λ and γ parameters increase while the values Du = 0.12, Sr = 0.5 are fixed for air. Fig. 8 illustrates the effects of Du on the fluid temperature. It can be clearly seen from this Figure that the diffusion thermal effects slightly affect the fluid temperature. As the values of Du increase, the fluid temperature decreases for water. The steady state concentration profiles are shown in Fig. 9 for the different values of thermal-diffusion (Sr). It shows that the increase in Sr leads to an increase in the value of concentration with time decreasing. It is to be noted that, for the value Sr = 2.0, the concentration increases very close to the wall, and decreases monotonically to reach zero. The concentration reaches the temporal maximum at the same value of Sr.

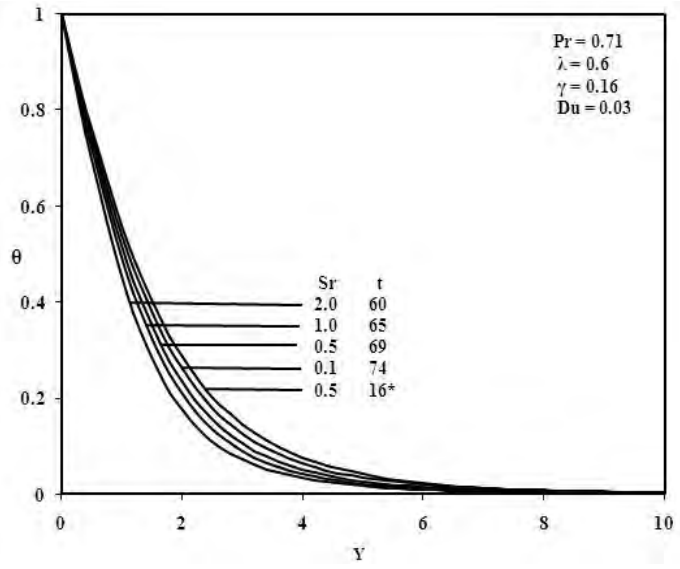

Fig. 5: Steady state temperature profiles for different values of Sr (*Temporal maximum)

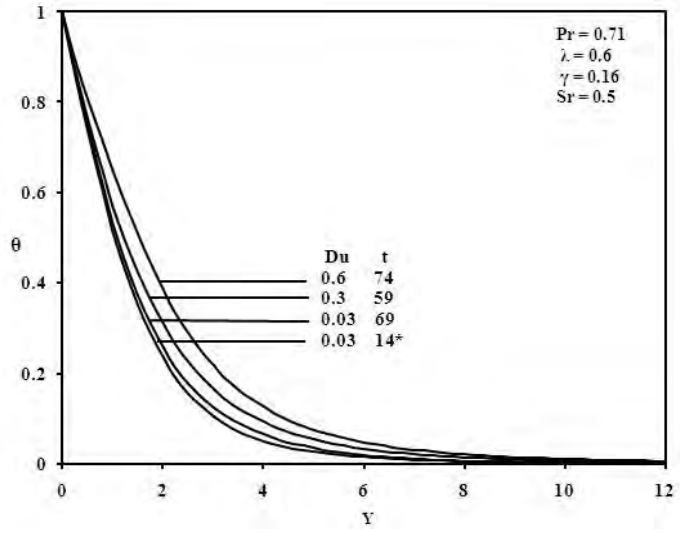

Fig. 6: Steady state temperature profiles different values of Du (*Temporal maximum)

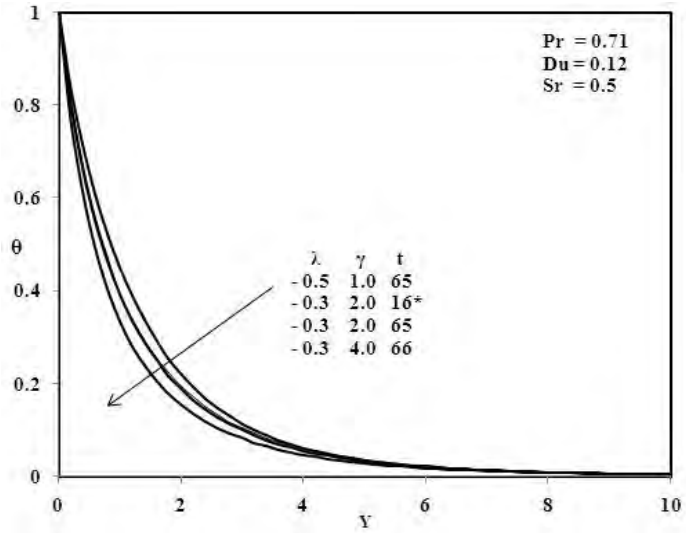

Fig. 7: Steady state temperature profiles for different values of λ and γ (*Temporal maximum)

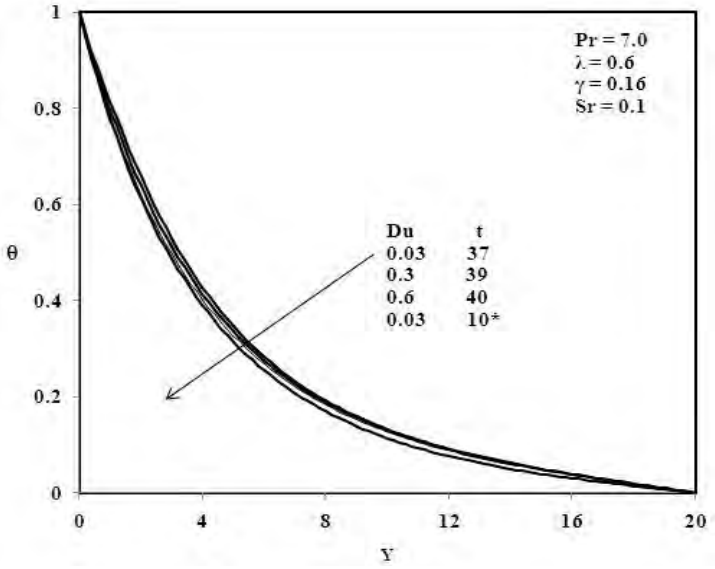

Fig. 8: Steady state temperature profiles for different values of Du (*Temporal maximum)

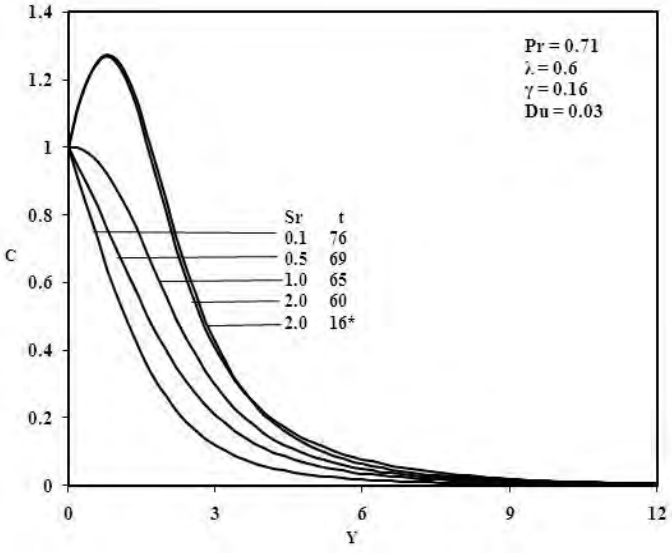

Fig. 9: Steady state concentration profiles for different values of Sr (*Temporal maximum)

Knowing the velocity, temperature and concentration field, it is customary to study the physical quantities of fundamental interest of the skin-friction, the rate of heat transfer and rate of concentration in state conditions. The local as well as average values of skin friction, Nusselt number and Sherwood number in dimensionless form are as follows:

The shear stress at the plate is defined as $\tau_w = \left(\mu \frac{\partial u}{\partial y} \right)_{y=0}$ (13)

Introducing non-dimensional variables in equation (13), we get $C_f = exp(-\lambda\theta) Gr^{3/4} \left(\frac{\partial U}{\partial Y} \right)_{Y=0}$

Considering $\frac{\nu \mu_\infty}{L^2}$ being the characteristic shear stress, then the non-dimensional form of local skin friction is obtained as $C_f = exp(-\lambda\theta) Gr^{3/4} \left(\frac{\partial U}{\partial Y} \right)_{Y=0}$ (14)

The average skin friction is $\overline{C_f} = exp(-\lambda\theta) Gr^{3/4} \int_0^1 \left(\frac{\partial U}{\partial Y} \right)_{Y=0} dX$ (15)

The local Nusselt number is defined by $N u_x = -L \left(k \frac{\partial T}{\partial y} \right)_{y=0} \Big/ k_\infty (T_w - T_\infty)$ (16)

Using the non-dimensional variables in equations (6) and (7), the non-dimensional form of local Nusselt number can be written as follows $Nu_X = -(1+\gamma\theta) Gr^{1/4} \left(\frac{\partial \theta}{\partial Y} \right)_{Y=0}$ (17)

The average Nusselt number can be written as follows $\overline{Nu} = -(1+\gamma\theta) Gr^{1/4} \int_0^1 \left(\frac{\partial \theta}{\partial Y} \right)_{Y=0} dX$ (18)

The Sherwood number is defined by $Sh_x = -x \left(\frac{\partial c'}{\partial y} \right)_{y=0} \Big/ C'_w - C'_\infty$ (19)

Using the non-dimensional variables in equation (6), the non-dimensional form of local Sherwood number can be written as $Sh_X = -XGr^{1/4} \left(\frac{\partial C}{\partial Y} \right)_{Y=0}$ (20)

The average Sherwood number is $\overline{Sh_X} = -Gr^{1/4} \int_0^1 \left(\frac{\partial C}{\partial Y} \right)_{Y=0} dX$ (21)

The derivations involved in Equations (13) to (21) are evaluated using a five point approximation formula and the integrals are evaluated using the Newton's cotes formula numerically.

It is observed that, an increase in the Prandtl number leads to a decrease in the value of the skin-friction coefficient. It is also observed from Fig. 10 that the skin friction increases with an increase in the Sr for Pr value of air, while the skin friction increases with an increase in the value of both λ and γ parameters for Pr value of water. From Fig. 11 it is observed that, an increase in the Prandtl number leads to a decrease in the value of the heat transfer coefficient in terms of the Nusselt number (Nu). It can be seen from the same Figure that the heat transfer coefficient increases with an increase in the Sr for the Pr value of air, while the heat transfer coefficient decreases as increase in the value of both Du and Sr for the Pr value of water.

The mass transfer coefficient in terms of the Sherwood number (Sh) for different values of Prandtl value is shown in Fig. 12. It represents the increase in the value of the Prandtl number and for the fixed values of Du = 0.03, λ = 0.6 and γ = 0.16 lead to increase the mass transfer coefficient. The mass transfer coefficient decreases with an increase in the value of Sr for both the values of the Prandtl number for air and water.

Fig.13 shows that for all the dimensionless parameters, the average skin friction increases monotonically, attains the temporal maximum and after some fluctuations reaches the steady state value. The average skin friction increases at small values of time *t* whereas at large values of *t*, it remains independent of *t*, i.e. the

average skin friction depends on time *t* only when *t* is small. As Sr increases, the average skin friction also increases.

Fig. 14 shows that, the average Nusselt number decreases sharply at small values of time *t*, being unaffected by Sr, but at large values of *t*, it is independent of time. When time increases, the average Nusselt number increases and after some fluctuations, and reaches the asymptotic steady state. Fig. 15 shows the average Sherwood number for different values of λ and γ with fixed values of Pr = 7.0, Du = 0.12, Sr = 0.5. It can be seen that the average Sherwood number decreases and increases suddenly, again increases and after some fluctuations, reaches the steady state. The average Sherwood number is also not affected by the parameters λ and γ at small values of *t*.

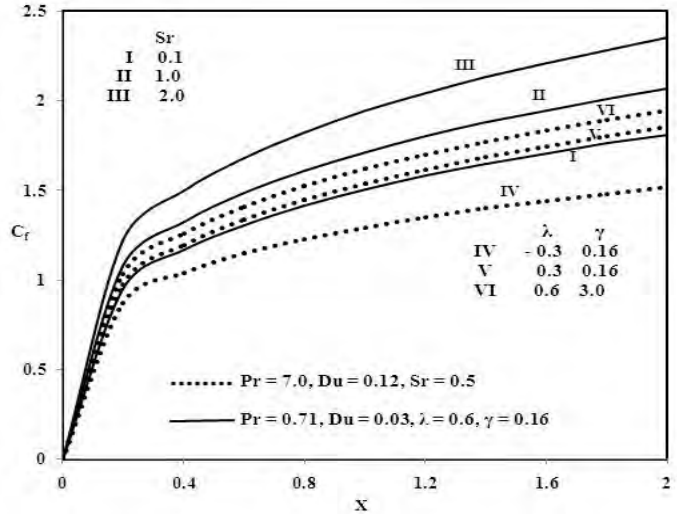

Fig. 10: Local skin friction

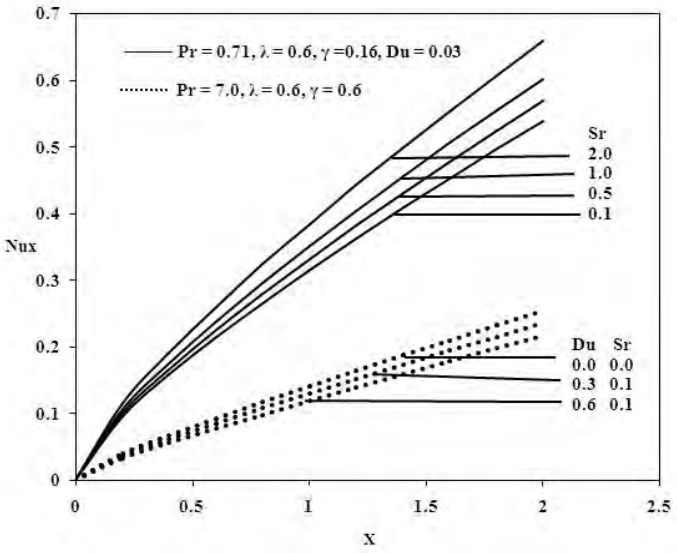

Fig. 11: Local Nusselt Number

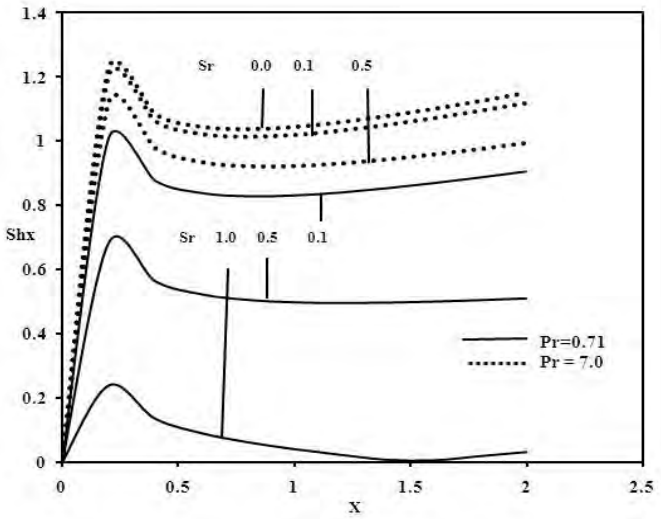

Fig. 12: Local Sherwood number

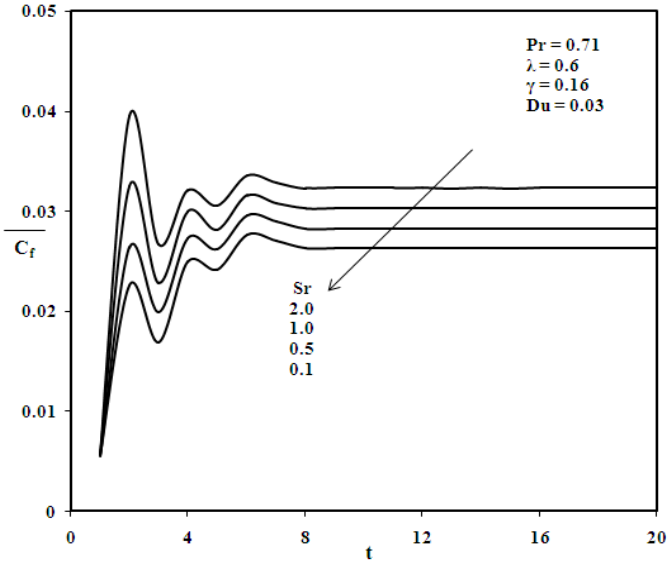

Fig. 13: Average skin friction

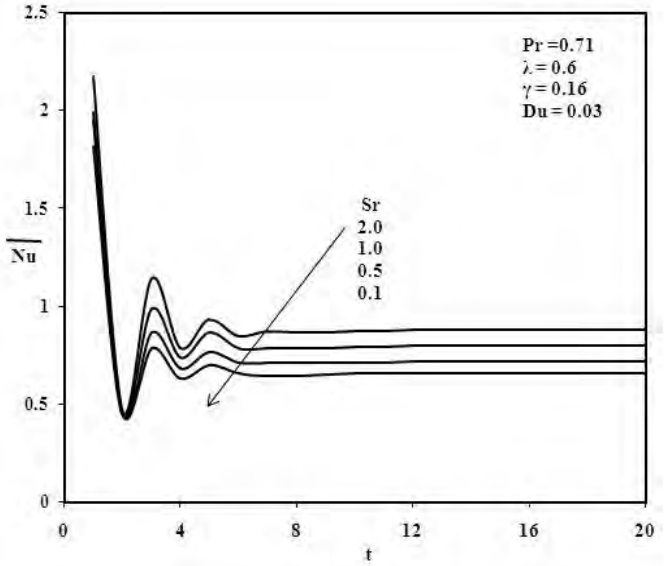

Fig. 14: Average Nusselt number

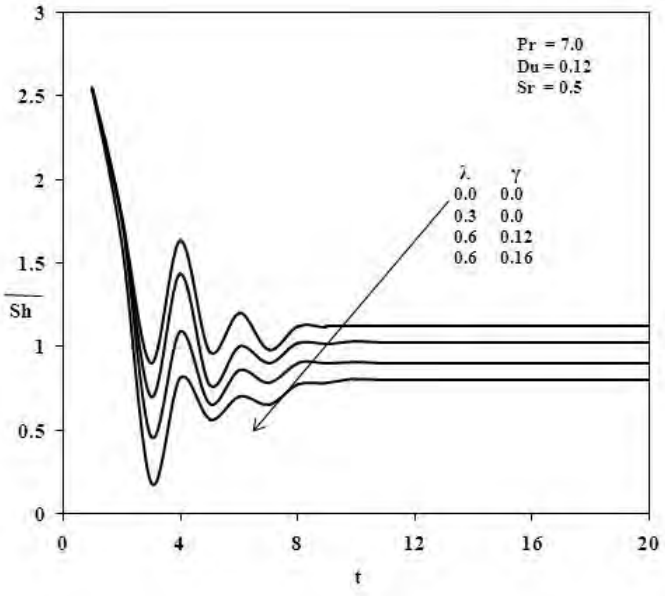

Fig. 15: Average Sherwood number

V. CONCLUSIONS

In this analysis, the problem of the Dufour and Soret effects on the unsteady free convective flow past a semi-infinite vertical plate in the presence of variable viscosity and thermal conductivity is considered, and it is solved by implicit finite-difference method of the Crank-Nicolson type. This analysis concludes with the following results:

The velocity increases with an increase in the Du and Sr numbers. The temperature decreases with an increase in Sr, variable viscosity and thermal conductivity parameters, with increasing time for air. But the temperature decreases as Du increases with time increasing for water.

The concentration profiles increase with an increase of the Sr number, while decreases with an increase of Du as time increases for air. The concentration profiles decrease with an increase of Du as time decreases for water. The local skin friction coefficient increases on increasing the value of Sr, variable viscosity and thermal conductivity parameters for both air and water. The local Nusselt number increases with Du, Sr numbers increase for both air and water.

Nomenclature

C'	concentration
C'_w	concentration near the plate
C	dimensionless concentration
C'_∞	concentration in the fluid far away from the plate
$\overline{C_f}$	average skin-friction coefficient
C_s	concentration susceptibility
C_f	skin-friction coefficient
C_p	specific heat at constant temperature
D_m	the mass diffusivity
Du	Dufour number
g	acceleration due to gravity
Gr	Grashof number
k	thermal conductivity
k_T	thermal diffusion ratio
L	length of the plate

Pr	Prandtl number
Sc	Schmidt number
Sr	Soret number
t'	time
t	dimensionless time
T	temperature of the fluid in the boundary layer
T_∞	ambient fluid temperature
T_w	plate temperature
T_m	mean fluid temperature
u, v	x and y component velocities respectively
U, V	X and Y component velocities respectively
x, y	dimensional coordinates along and normal to the plate
X, Y	dimensionless coordinates along and normal to the plate
Sh_x	Sherwood number
$\overline{Sh}$	Average Sherwood number
N	Buyoancy ratio
Nu_X	Local Nusselt number
$\overline{Nu}$	average Nusselt number

Greek symbols

β	coefficient of volume expansion
β^*	coefficient of concentration expansion
γ	thermal conductivity variation parameter
λ	viscosity variation parameter
μ	fluid viscosity
μ_∞	fluid viscosity in free stream
υ	kinematic viscosity
ρ	density
θ	dimensionless temperature

Subscripts

w	condition of the wall
∞	free stream condition

REFERENCES

[1] Sparrow, E. M., Minkowycz, W. J., and Eckert, E. R. G., Diffusion-thermo effects in stagnation- point flow of air with injection of gases of various molecular weights into the boundary layer, AIAAJ, Vol. 2, 652–659, 1964.

[2] Gnaneswara Reddy, M., and Bhaskar Reddy, N., Soret and Dufour effects on steady MHD free convection flow past a semi-infinite moving vertical plate in a porous medium with viscous dissipation, International Journal of Applied Mathematics and Mechanics, Vol. 6(1), 1-12, 2010.

[3] Alam, M. S., Rahman, M. M., Maleque, A., and Ferdows, M., Dufour and Soret effects on steady MHD combined free-forced convective and mass transfer flow past a semi-infinite vertical plate, International Journal of Science and Technology, Vol. 11(12), 1-12, 2006.

[4] Kafoussias, N. G. and Williams, E. W., Thermal-diffusion and diffusion-thermo effects on mixed free forced convective and mass transfer boundary layer flow with temperature dependent viscosity, International Journal of Engineering Science, Vol. 33(9), 1369–1384, 1995.

[5] Postelnicu, A., Influence of a magnetic field on heat and mass transfer by natural convection from vertical surfaces in porous media considering Soret and Dufour effects, International Journal of Heat and Mass Transfer, Vol. 47(6-7), 1467–1472, 2004.

[6] Alam, M. S., Ferdows, M., Ota, M., and Maleque, M. A., Dufour and Soret effects on steady free convection and mass transfer flow past a semi-infinite vertical porous plate in a porous medium, International Journal of Applies Mechanics Engineering, Vol. 11(3), 535–545, 2006.

[7] Hayat, T., Mustafa, M., and Pop, I., Heat and mass transfer for Soret and Dufour's effect on mixed convection boundary layer flow over a stretching vertical surface in a porous medium filled with a viscoelastic fluid, Communications in Nonlinear Science and Numerical Simulation, Vol. 15(5), 1183–1196, 2010.

[8] Srinivasacharya, D and Ram Reddy, Ch., Mixed convection heat and mass transfer in a micropolar fluid with Soret and Dufour effects, Advanced Applied Mathematics and Mechanics, Vol. 3, 389-400, 2011.

[9] Kafoussias, N. G., and Williams, E. W., The effect of temperature-dependent viscosity on the free convective laminar boundary layer flow past a vertical isothermal flat plate, Acta Mechanica, Vol. 110, 123-137, 1995.

[10] Hady, F. M., Bakier, A. Y., and Gorla, R. S. R., Mixed convection boundary layer flow on a continuous flat plate with variable viscosity, Heat and Mass Transfer, Vol. 31(3), 169-172, 1996.

[11] Emad M. Abo-Eldahab., and Aahmed M. Salem., Radiation effect on MHD free convection flow of a gas past a semi-infinite vertical plate with variable viscosity, International Journal of Computational Fluid Dynamics, Vol. 14(3), 243-252, 2001.
[12] Seddeek, M. A., The effect of variable viscosity on hydromagnetic flow and heat transfer past a continuously moving porous boundary with radiation, International Communications in Heat and Mass Transfer, Vol. 27(7), 1037-1046, 2000.
[13] Hossain, M. A., Khalil Khanafer., and Kambiz vafai., The effect of radiation on free convection flow of fluid with variable viscosity from a porous vertical plate, Int. J. Therm. Science, Vol. 49, 115-124, 2001.
[14] Elbarbary, E. M. E., and Elgazery, N. S., Chebyshev finite difference method for the effects of variable viscosity and variable thermal conductivity on heat transfer from moving surfaces with radiation, International Journal of Thermal Science, Vol. 43, 889-899, 2004.
[15] Rahman, M. M., Mamun, A. A., Azim, M. A., and Alim, M.A., Effects of temperature dependent thermal conductivity on magneto hydrodynamic (MHD) free convection flow along a vertical flat plate with heat conduction, Nonlinear Analysis Modelling and Control, Vol. 13(4), 513–524, 2008.
[16] Mahanti, N. C., and Gaur, P., The effects of varying viscosity and thermal conductivity on steady free convective flow and heat transfer along an isothermal vertical plate in the presence of heat sink, Journal of Applied Fluid Mechanics, Vol. 2(1), 23-28, 2009.
[17] Eckert, E. R. G., and Robert M. Drake., Heat and Mass transfer, McGraw-Hill, New York, 1963.
[18] Schlichting, H., Boundary Layer Theory, Mc Graw-Hill, New York, 1979.
[19] Elbashbeshy, E. M. A., and Ibrahim, F. N., Steady free convection flow with variable viscosity and thermal diffusivity along a vertical plate, Journal of Physics D: Applied Physics, Vol. 26(12), 2137-2143, 1993.
[20] Ockendon, H., and Ockendon, J. R., Variable viscosity flows in heated and cooled channels, Journal of Fluid Mechanics, Vol. 83, 177-190, 1977.
[21] Ramachandra Prasad, V., Bhaskar Reddy, N., and Muthucumaraswamy, R., Radiation and mass transfer effects on two-dimensional flow past an impulsively started infinite vertical plate, International journal of Thermal Sciences, Vol. 46, 1251-1258,2007.
[22] Carnahan, B., Luther, H. A., and Wilkes, J. O., Applied Numerical Methods, Wiley, New York, 1969.
[23] Soundalgekar, V. M., and Ganesan, P., Finite difference analysis of transient free convection with mass transfer of an isothermal vertical flat plate, International Journal of Engineering Science, Vol. 19, 757-770, 1981.

AUTHOR PROFILE

P. LOGANATHAN received M.Sc degree from Presidency College, Chennai and M.Phil. from Loyola College, Chennai. He also received a Ph.D. degree in Mathematics from Anna University, Chennai, India. He is working as a Professor in the Department of Mathematics, Anna University. His areas of interest are Computational Fluid Dynamics, Heat and Mass transfer and Object Oriented Programming. He has published about 40 papers in national and international journals

D. IRANIAN obtained M.Sc degree from C.P.A College, Bodi and M.Phil. from Saraswathi Narayanan College, Madurai. He received Ph.D. degree in Mathematics in the area of Computational Fluid Dynamics from Anna University, Chennai, India. He is working as a Professor in the Department of Mathematics, Panimalar Institute of Technology, Chennai. He has published 3 international papers.

P. GANESAN received Ph.D. degree in Mathematics from IIT, Bombay, India. He has more than 30 years of teaching experience and worked as Professor in the Department of Mathematics, Anna University, Chennai, India. His areas of interest are Computational Fluid Dynamics, Heat and Mass transfer. He has published about 56 papers in national and international journals.